Thermoelastic properties of perfect crystals with nonprimitive lattices. II. Application to KCl and NaCl

L. N. Kantorovich*
Departamento de Quimica Fisica y Analitica, Universidad de Oviedo, 33006 Oviedo, Spain
(Received 18 April 1994; revised manuscript received 9 August 1994)

In Part I, the theory for external and internal strain derivatives of the Helmholtz free energy of a perfect crystal was developed in the quasiharmonic approximation. The theory allows us to consider arbitrary piezoelectric shell-model-like crystals at any temperature and under general external stress conditions. In the present part of this work we show how these derivatives can be utilized in the simplest way in order to calculate a wide range of macroscopic thermoelastic properties of the crystals. The method was realized in a computer code written without additional artificial constraints concerning crystal symmetry and structure. Special attention is paid to the numerical implementation of the formulas obtained. Using different types of pair potentials including *ab initio* ones, various elastic, dielectric, and general thermodynamic properties of KCl and NaCl crystals are calculated here for a wide range of temperatures and pressures (only for NaCl). Our calculations in the vicinity of the melting point demonstrate that the free energy has a minimum which disappears at some critical temperature, and the transition is controlled only by the isothermal elastic constant C_{11}^T. It decreases so catastrophically rapidly with increase of temperature that it leads to an immediate violation of the stability condition $C_{11}^T > C_{12}^T$ before the isothermal bulk modulus reaches zero. The calculations also clearly show that the empirical pair potentials of Catlow *et al.* are in reasonably good agreement with most of the experimental data. In addition, we show, in accord with other authors, that the quasiharmonic approximation can be successfully used almost up to half of the crystal melting temperature, although physically correct qualitative results could be expected even near the melting point.

I. INTRODUCTION

In part I of this work[1] (referred to hereafter as I), we have developed a general theory for the Helmholtz free-energy derivatives with respect to both external and internal strains within the quasiharmonic approximation when only the first (major) term in the thermodynamic perturbation theory[2,3] is left. An arbitrary piezoelectric crystal was considered no matter what structure and symmetry it has. The crystal potential energy used in the derivation was chosen from the theory of deformable dipoles developed by Tolpygo *et al.*[4] The method incorporates electronic coordinates of the crystal in the form of shells allowing for account to be taken of both the electronic polarization and correct behavior of the optical phonon branches. It is worthwhile to mention here that this model, although physically equivalent and similar to the widely applied shell models,[5–8] is not identical to them.

The theory has been implemented in a computer code written in a general way allowing for arbitrary crystal structure and symmetry as well as a sufficiently general form of the pair potential between cores and shells of atoms. In this paper we report our first numerical results calculated using this computer code. So, the main objectives of the present paper are (i) to pay special attention to the most efficient numerical implementation of the formulas for the free-energy derivatives obtained in I; (ii) to consider a wide range of thermodynamic, dielectric, and elastic properties of KCl and NaCl crystals, using several well-known pair potentials over a wide range of temperatures and pressures and to make a thorough comparison of the results with available experimental data; (iii) to study crystal stability near the melting point and the mechanism which leads crystals to melt.

These alkali halides were chosen pursuing several purposes. First of all, a lot of experimental information on the temperature and pressure dependencies of their elastic and dielectric properties obtained by different experimental techniques is available. On the other hand, because of their simplicity, these alkali halides have always been a preferred model system on which theoreticians could check and polish their theories. For that reason, a number of theoretical works on the subject performed by various methods are also available[9–14] for comparison with our numerical results.

The plan of the paper is the following. In Sec. II the usage of the crystal symmetry while performing the Brillouin zone (BZ) integration by the special points method[15] is considered. In Sec. III, we give a short outline of properties which are calculated from the free-energy derivatives. Several details of our calculations are described in Sec. IV. Various zero-pressure thermoelastic are dielectric properties of NaCl and KCl rock-salt crystals for a wide range of temperatures are considered in Sec. V. For the NaCl crystal we also study the pressure dependence of its several mechanical properties. Special attention in this section is also paid to the mechanism of melting observed in our numerical simulations. The main conclusions are made in Sec. VI. For the reader's con-

venience we have preserved all notations used in I. Every reference to the equation (N) presented in I is made here as (IN).

II. INTEGRATION OVER THE BRILLOUIN ZONE

The contributions to the Helmholtz free-energy derivatives considered in I should be calculated independently for every vector $\mathbf{k}\in$BZ. In this section we shall perform a proper symmetry analysis in order to show how to reduce all $\mathbf{k}$ points to the irreducible part of the BZ in our case.

Let us consider a sublattice s with a vector $\mathbf{X}(s)$ in the 0th unit cell (UC). Under some element $\hat{g}=[\hat{f}|\tau_f+\mathbf{R}(l)]$ of the space group $\mathfrak{G}$ of the crystal this sublattice is transformed to another one or to the same sublattice. This target sublattice will be marked hereafter as $s(g)$. In addition, the following notation will be used in this section: $\hat{f}$ is an element of the crystal point group (so-called crystal class) corresponding to some $\hat{g}\in\mathfrak{G}$, while τ_f is the accompanying fractional translation. We shall not use here the direct lattice translations $\mathbf{R}(l)$ since they do not affect the properties in question. Thus, we can restrict ourselves to considering a set of elements $\{(\hat{f}|\tau_f)\}$. We shall use the same symbol $\mathfrak{G}$ for this set as for the space group. For symmorphic crystals $s(g)\equiv s$, though for nonsymmorphic ones there is always at least one such element $\hat{g}\in\mathfrak{G}$ that produces a sublattice $s(g)\neq s$.

If we examine carefully the definition of the dynamical matrix, $\Omega^{ss'}_{\alpha\alpha'}(\mathbf{k})$ [see equations which follow after Eq. (I.10) in Sec. II B of I], we can recognize that it is the Fourier transform [shown explicitly by Eq. (I.11), for instance] of a matrix $\Omega^{ss'}_{\alpha\alpha'}(\mathbf{R})$ defined in the direct space. This matrix behaves as a product of vectors $R_\alpha R_{\alpha'}$. That is why for any point-group operation $\hat{f}$ (except those for which $\hat{f}^{-1}\mathbf{k}=\mathbf{k}$) the matrix $\Omega(\hat{f}^{-1}\mathbf{k})=\|\Omega^{ss'}_{\alpha\alpha'}(\hat{f}^{-1}\mathbf{k})\|$ is transformed by means of the following similarity transformation:

$$\Omega(\hat{f}^{-1}\mathbf{k})=\Phi(g)\Omega(\mathbf{k})\Phi(g)^\dagger , \tag{1}$$

where $\hat{g}=(\hat{f}|\tau_f)\in\mathfrak{G}$. The transformation matrix $\Phi(g)=\|\Phi^{ss'}_{\alpha\alpha'}(g)\|$ (cf. Ref. 7) is given by

$$\Phi^{ss'}_{\alpha\alpha'}(g)=C_{\alpha\alpha'}(f)\delta_{s',s(g)} . \tag{2}$$

It contains a matrix $\mathbf{C}(f)=\|C_{\alpha\alpha'}(f)\|$ of the three-dimensional point-group operation, $\hat{f}$. As the result of the transformation (1), the eigenvalues $\lambda_{\mathbf{k}j}=\omega^2_{\mathbf{k}j}$ of the dynamical matrix are not changed while the corresponding eigenvectors are transformed as

$$\mathbf{e}(\hat{f}^{-1}\mathbf{k},j)=\Phi(g_0)\mathbf{e}(\mathbf{k}j) , \tag{3}$$

where $\hat{g}_0\in\mathfrak{G}$ is used instead of $\hat{g}$ because if $\mathbf{k}$ lies on the BZ surface, it may happen that $\hat{f}^{-1}\mathbf{k}=\mathbf{k}'+\mathbf{g}$, where $\mathbf{g}$ is a reciprocal-lattice vector, $\mathbf{k}'\in$ BZ. In the latter case $\hat{g}_0=(\hat{f}_0|\tau_{f_0})$ gives just the vector $\mathbf{k}'$, i.e., $\hat{f}_0^{-1}\mathbf{k}=\mathbf{k}'$. In all other cases $\hat{g}_0=\hat{g}$.

The integrals over the BZ (over $\mathbf{k}$) are calculated using the special point method, i.e., employing the recipe[15]

$$\frac{1}{N}\sum_{\mathbf{k}} f(\mathbf{k})=\sum_{a} W_a \frac{1}{|\mathfrak{G}|}\sum_{\hat{g}\in\mathfrak{G}} f(\hat{f}^{-1}\mathbf{k}_a) , \tag{4}$$

where $|\mathfrak{G}|=\dim\mathfrak{G}$ and $f(\mathbf{k})$ is any smooth-enough function defined in the BZ, and the index a runs over the special points $\mathbf{k}_a$ lying in the irreducible part of the BZ, W_a are the corresponding weighting factors. The second summation in Eq. (4) is carried out over all operations of the set $\mathfrak{G}$, i.e., over all the point-group operations.

In practice, we encounter two major problems in trying to implement Eq. (4). First of all, every function $f(\mathbf{k})$ staying under the summation sign should be smooth enough to be easily integrated by means of this finite term quadrature. Examining carefully all derivatives given by Eqs. (I.54) and (I.55), we showed that it is so in our case.

The second problem deals with the second summation (over the point-group elements) in Eq. (4). We are going to show that we can restrict ourselves to the calculation of the free-energy derivatives exclusively at a limited number of special points $\{\mathbf{k}_a\}$, distributed over the irreducible part of the BZ.

Actually, our task is to link $\mathfrak{F}_{\mathbf{k}j}$ derivatives calculated at different points $\mathbf{k}$ belonging to the same star, $\hat{f}^{-1}\mathbf{k}$. For that purpose, we must derive corresponding symmetry properties of $\Delta^{jj'}_{r'r''}(\mathbf{k}|x_i)$ and $\Delta^{jj}_{r'r''}(\mathbf{k}|x_i,x_{i'})$ defined and obtained in Sec. III C of I. Here x_i and $x_{i'}$ mean either external, $(\beta\gamma)$, or internal,

$$\mathrm{u}\begin{bmatrix} s \\ \sigma \end{bmatrix} ,$$

strains.

Let us consider first $\tilde{\Delta}^{jj'}(\mathbf{k}|\beta\gamma)$ given by Eqs. (I.73) and (I.75). It follows from Eqs. (I.77), (I.79), (I.80), and (I.89) that the matrix $B^{ss'}_{\alpha\alpha'}(\mathbf{k}|\beta\gamma)=\partial B^{ss'}_{\alpha\alpha'}(\mathbf{k})/\partial u_{\beta\gamma}$ behaves as a fourfold product of vectors $R_\alpha R_{\alpha'} R_\beta R_\gamma$. Thus we get

$$\mathbf{B}(\hat{f}^{-1}\mathbf{k}|\beta\gamma) = \Phi^\dagger(g_0)\left[\sum_{\beta_1\gamma_1} C_{\beta\beta_1}(f_0)C_{\gamma\gamma_1}(f_0)\mathbf{B}(\mathbf{k}|\beta_1\gamma_1)\right]\Phi^\dagger(g_0) . \tag{5}$$

Apparently, the same properties hold for the matrices $\mathbf{A}(\hat{f}^{-1}\mathbf{k}|\beta\gamma)$ and $\mathbf{D}(\hat{f}^{-1}\mathbf{k}|\beta\gamma)$ constituting other components of the dynamical matrix, see I for details. Using these results we conclude that the vectors $\psi(\mathbf{k}j)$, Eq. (I.71), are transformed in the same way as the vectors $\mathbf{e}(\mathbf{k}j)$, i.e., by means of Eq. (3), whereas the vectors $\mathbf{f}_j(\mathbf{k}|\beta\gamma)$, Eq. (I.72), are transformed as

$$\mathbf{f}_j(\hat{f}^{-1}\mathbf{k}|\beta\gamma)=\Phi(g_0)\left[\sum_{\beta_1\gamma_1} C_{\beta\beta_1}(f_0)C_{\gamma\gamma_1}(f_0)\mathbf{f}_j(\mathbf{k}|\beta_1\gamma_1)\right] . \tag{6}$$

Therefore, using Eqs. (I.73) and (I.75), we get the following result:

$$\Delta^{jj'}(\hat{f}^{-1}\mathbf{k}|\beta\gamma) = \sum_{\beta_1\gamma_1} C_{\beta\beta_1}(f_0)C_{\gamma\gamma_1}(f_0)\Delta^{jj'}(\mathbf{k}|\beta_1\gamma_1) . \tag{7}$$

In deriving the last equation, we have made use of the identity $\Phi^{\dagger}\Phi=1$ since the matrix $\Phi(g_0)$ is unitary.

All other symmetry properties can be established in the same way. The internal strain derivatives of the matrices $\mathbf{A}(\mathbf{k})$, $\mathbf{B}(\mathbf{k})$, and $\mathbf{D}(\mathbf{k})$ behave as a three-fold product $R_{\alpha}R_{\alpha'}R_{\sigma}$ and, therefore, are transformed adequately. As a result, we get in this case

$$\Delta^{jj'}\left[\hat{f}^{-1}\mathbf{k}|_{\sigma}^{s}\right]=\sum_{\sigma_1}C_{\sigma\sigma_1}(f_0)\Delta^{jj'}(\mathbf{k}|_{\sigma_1}^{s(g)}) . \tag{8}$$

Note that in the last equation we have a symmetry-related sublattice $s(g)$ [instead of s as it was in Eq. (7)] on the right-hand side. That is why, in the general case of nonsymmorphic crystals, we must know the complete set $\mathfrak{G}$ of the space-group generators as pairs of the point-group elements and accompanying fractional translations.

In order to find the bracket $\{\beta\gamma\}_T$ given by Eqs. (I.50) we must apply the recipe of Eq. (4) to the corresponding functions in Eq. (I.54). Then we must express the first-order derivatives of $\lambda_{\mathbf{k}'j}$, (where $\mathbf{k}'=\hat{f}^{-1}\mathbf{k}$) with respect to the external strains through those calculated at the point $\mathbf{k}$ (for any $\hat{f}$). These derivatives are eigenvalues of Eq. (I.69). Since the eigenvectors $C_r^{(jr)}(\mathbf{0})$ in Eq. (I.69) do not depend on the particular strain component $(\beta\gamma)$ in question, the eigenvalues just repeat the transformation suffered by the matrix $\Delta^{jj'}(\hat{f}^{-1}\mathbf{k}|\beta\gamma)$ itself. Thus, we can write down the following final result making use of Eqs. (I.50), (I.54), (4), and (7):

$$\{\beta\gamma\}_T=\sum_a W_a\phi_2(\omega_{\mathbf{k}_a}j)\sum_{\beta_1\gamma_1}\left[\frac{1}{|\mathfrak{G}|}\sum_{\hat{g}\in\mathfrak{G}}C_{\beta\beta_1}(f_0)C_{\gamma\gamma_1}(f_0)\left[\frac{\partial}{\partial u_{\beta_1\gamma_1}}\lambda_{\mathbf{k}_a j}\right]_0\right] . \tag{9}$$

We obtained for the internal strain brackets in the same manner:

$$\begin{Bmatrix}s\\ \sigma\end{Bmatrix}_T=\sum_a W_a\phi_2(\omega_{\mathbf{k}_a}j)\sum_{\sigma_1}\left[\frac{1}{|\mathfrak{G}|}\sum_{\hat{g}\in\mathfrak{G}}C_{\sigma\sigma_1}(f_0)\left[\frac{\partial}{\partial u\begin{Bmatrix}s(g)\\ \sigma_1\end{Bmatrix}}\lambda_{\mathbf{k}_a}j\right]_0\right] . \tag{10}$$

All second-order brackets represented by Eqs. (I.51)–(I.53) can be considered analogously. Thus, actual calculations should be carried out only in the irreducible part of the BZ.

III. CALCULATION OF THERMODYNAMIC PROPERTIES OF A CRYSTAL FROM THE FREE-ENERGY DERIVATIVES

The theory presented so far allows one to calculate dielectric and isothermal second-order elastic properties of an arbitrary perfect crystal provided that pair potentials between atoms are known. The following material constants of any crystal can be evaluated for any given configuration of the crystal [i.e., for any set of basic direct lattice vectors $\mathbf{a}_1$, $\mathbf{a}_2$, $\mathbf{a}_3$, and sublattice vectors $\mathbf{X}(s)$]: static dielectric tensor, from the static susceptibility, $\chi_{\alpha\beta}(0)$, see Eq. (I.45); static direct (=converse) piezoelectric tensor, Eq. (I.44) and isothermal elastic constants, $C^T_{\beta\gamma,\beta'\gamma'}$, Eq. (I.47). The high-frequency constants can also be obtained making use of Eqs. (I.44) and (I.45), except all matrices are considered only on the subspace of the shell coordinates (cf. Ref. 16).

The complete set of brackets

$$\begin{Bmatrix}s\\ \sigma\end{Bmatrix}=\begin{Bmatrix}s\\ \sigma\end{Bmatrix}_{\rm st}+\begin{Bmatrix}s\\ \sigma\end{Bmatrix}_T$$

shows if the crystal is in equilibrium with respect to the internal strains for the configuration under consideration. Finally, the initial stress tensor $\tau^0_{\beta\gamma}$. Eq. (I.46), shows to which external conditions (i.e., to which external mechanical forces) this particular structure should correspond.

The next step would be to compare the properties calculated with those obtained experimentally. However, as far as the elastic properties are concerned, we have to notice that it is the adiabatic elastic constants or stiffnesses[5] that are usually available in the literature. It was shown in Ref. 5 and 17, how that (as well as some other thermodynamic properties) can be obtained from the isothermal free-energy derivatives, and so we omit this point here.

IV. SOME DETAILS OF THE CALCULATIONS

First we point out that while making calculations at different crystal spacings (for example, for a set of zero-pressure equilibrium structures at different T) special care should be taken to include a sufficient number of neighbors in the summations over the lattice and to avoid possible discontinuities in the free energy. In other words, the precision of the lattice summations should be increased as the spacings become larger. This is especially important at rather high T.

We have used the Monkhorst-Pack homogeneous mesh of points[18] in the whole BZ for generating a set of special points. In order to avoid singularities in the summations sets containing the $\mathbf{k}=\mathbf{0}$ point were disregarded. Then, using symmetry operators of the space group of the crystal, only $\mathbf{k}$ vectors lying in the irreducible part of the BZ are evaluated, $\{\mathbf{k}_a\}$, and the corresponding weighting factors, $\{W_a\}$, are computed. In fact, the final number of special points, $\{\mathbf{k}_a\}$, depends not only on the MP parameter, $q_{\rm MP}$,[18] but also on the crystal point group. As fol-

lows from Sec. II, all actual calculations are carried out only for this set of **k** points, $\{\mathbf{k}_a\}$.

In Table I, our results for a set of KCl properties versus number of **k** points in the irreducible part of the BZ for two different temperatures (200 and 800 K) are given. These calculations were carried out using empirical pair potentials of Catlow *et al.*[19] with parameters of shells which will be described below. Note that in our calculations these pair potentials act between cores of atoms. It is seen that 10 special points are sufficient for almost all the properties studied and listed in Table I. However, the elastic constants C_{12}^T and C_{12}^S were found to be much more sensitive to the number of **k** points in the BZ used in the calculations, so that in these cases the error is larger and lies between 2 and 8 %. Note that the error increases as the temperature goes up.

In this paper, we consider several types of the core-core pairwise potentials for KCl and NaCl rock salts: (i) empirical pair potentials of Catlow *et al.*[19] fitted to experimental elastic and dielectric properties extrapolated to zero temperature (their set 1 potentials); (ii) empirical pair potentials of Tosi and Fumi[20] developed while analyzing the thermodynamic data; (iii) *ab initio* PI pair potentials[21] from *ab initio* perturbed ion[22] (*ab*PI) calculations of these crystals. We should stress that we could not choose, for example, set 2 of the potentials of Catlow *et al.*[19] which lead to discontinuities[12] in the third- and the fourth-order derivatives of the free energy used here while calculating the derivatives of the phonon frequencies.

For every potential we have obtained appropriate shell parameters. This was done in the following way. First of all, we have ignored short-range shell-shell potentials $Z^{ss'}(R)$ in our calculations since they turned out to be not so important for the crystals studied. The polarizabilities of both cations and anions were chosen from theoretical predictions made in Ref. 23. They match quite well experimental high-frequency dielectric constants ε_∞ (Ref. 24) by means of the Clausius-Mosotti relation (Table II).

Here we have adopted a model in which only $\Gamma^{-+}(R)\neq 0$, i.e., when only the shell-core interaction between anions and cations is taken into account. This model works quite well for alkali halides[4] and simply means that induced polarization on the cations is negligibly small in comparison with that on the anions which have much more flexible electronic shells. The short-range potential $\Gamma^{-+}(R)$ was chosen to be of a one-exponential form $\Gamma^{-+}(R)=\Gamma e^{-\beta R}$. Its parameters Γ and β were obtained in a special set of calculations.

TABLE I. Properties of KCl crystal calculated using pair potentials (Ref. 19) with our shell parameters (see text) for the spacing (the anion-cation nearest-neighbor distance) $d=5.897$ a.u. versus number of special points in the BZ; $T=200$ (the first row) and $T=800$ (the second row).

Property	Number of points in the irreducible part of the BZ: 2	10	28	60	110	182	Δ[a]
$\varepsilon(0)$	4.639 17	4.608 55	4.607 39	4.606 97	4.605 96	4.605 84	0.06
	5.1431	4.972 96	4.966 91	4.964 65	4.959 29	4.958 67	0.29
	Heat capacities in cal K^{-1} mol^{-1}						
$C_\eta=C_v$	11.153 6	11.159 2	11.164 1	11.164 3	11.162 2	11.162 3	0.03
	11.872 8	11.873 2	11.873 6	11.873 6	11.873 4	11.873 4	0.00
$C_\tau=C_p$	11.528 0	11.483 5	11.487 8	11.486 7	11.481 6	11.481 3	0.02
	13.832 5	13.524 5	13.515 6	13.503 9	13.483 8	13.480 9	0.32
	Pressure, elastic constants, and bulk modulus in GPa (1 GPa$=10^{10}$ dyn/cm^2)						
P	0.258 12	0.232 40	0.232 57	0.232 00	0.230 31	0.230 21	0.95
	1.547 68	1.444 16	1.444 34	1.442 07	1.435 52	1.435 1	0.63
C_{11}^T	45.615 5	45.175 6	45.067 6	45.058 4	45.079 4	45.076 2	0.22
	39.880 9	38.119 2	37.685 9	37.649 1	37.733 7	37.720 8	1.06
C_{12}^T	6.011 31	6.562 45	6.655 15	6.689 73	6.709 23	6.719 68	2.34
	4.736 98	6.939 99	7.311 03	7.449 29	7.526 95	7.568 7	8.31
C_{44}^T	6.286 77	6.279 65	6.277 16	6.276 38	6.276 41	6.276 40	0.05
	5.844 74	5.816 35	5.806 59	5.803 57	5.803 66	5.803 61	0.22
C_{11}^S	46.263 2	45.742 5	45.634 0	45.623 1	45.639 5	45.636 0	0.23
	42.681 5	40.596 8	40.163 8	40.120 2	40.185 1	40.170 9	1.06
C_{12}^S	6.658 97	7.129 38	7.221 54	7.254 42	7.269 34	7.279 47	2.06
	7.537 59	9.417 59	9.788 92	9.920 33	9.978 35	10.018 8	6.00
B_T	19.298 7	19.511 0	19.536 8	19.556 6	19.576 1	19.581 9	0.36
	16.967 5	17.814 4	17.917 4	17.996 6	18.074 4	18.097 8	1.57
B_S	19.946 4	20.077 9	20.103 2	20.121 3	20.136 2	20.141 7	0.32
	19.768 1	20.292 1	20.395 3	20.467 6	20.525 8	20.547 9	1.24
	Thermal expansion in 10^{-4} K^{-1}						
β_T	10.528 5	9.745 73	9.730 39	9.705 98	9.655 99	9.650 39	0.99
	12.846 0	11.508 3	11.442 9	11.376 9	11.282 7	11.265 3	2.16

[a]The relative error (in %) in calculations involving 10 points with respect to those involving 182 points.

These were made for every crystal at zero temperature for experimental crystal spacings[25] in such a way as to fit the experimental[24] low-frequency dielectric constant, ε_0, and the transverse-optical (TO) frequency, $\omega_{0,\mathrm{op}\perp}$, at the Γ point ($\mathbf{k}=\mathbf{0}$) of the BZ. In this fitting, we have calculated the low-frequency dielectric constant, ε_0, by using only the static crystal energy since at $T=0$ the quasiharmonic contribution is almost negligible and can be omitted (see below).

The final set of shell parameters is presented in Table II together with corresponding crystal properties, both calculated and experimental. Note that our long-wavelength optical frequencies are in quite good agreement with the Lyddane-Sachs-Teller relation.[26] It is seen from Table II that the exponent β is almost unaffected by the form of the core-core part of the total crystal potential and the main difference lies in the value of Γ. Examining data in Table II we conclude that calculated and experimental values agree satisfactorily for all types of the pair potentials except for the case of the Tosi-Fumi potentials for which we could not achieve the experimental TO frequency using this form of the shell-core potential. The final potentials (with shells) obtained in this way will be called in this paper as ppCDN, PIpp, and TFpp in the cases of the pair potentials of Catlow *et al.*,[19] PI,[21] and of Tosi and Fumi,[20] respectively.

The formalism presented above was realized in a computer code DYNAM which allows one to calculate a wide range of thermoelastic and dielectric properties of any shell-like-model crystal for both arbitrary temperature and external mechanical stresses. Phonon curves in an arbitrary direction in the BZ as well as corresponding sound wave velocities can also be computed. All numerical results presented in this paper were obtained using this computer code.

Our formulas allow one to calculate the thermoelastic and dielectric properties of a crystal for some particular configuration. This means that calculations such as "a property versus pressure" for a set of desired temperatures can be done immediately. However, one encounters some difficulties if the temperature dependence of a property is needed for a set of given pressures. This is so because it is not known *a priori* to which structure these pressures and temperatures correspond.

In order to overcome this inconvenience and avoid quite tedious minimizations of the Gibbs free energy in every case, we made our calculations in the following way. At every temperature of interest we made calculations for a range of spacings in order to cover the desired range of pressures. Then, a linear interpolation was made in order to obtain equilibrium spacings. These calculations have been done with 10 special points. Then we have carried out a set of individual calculations with 28 special points for these particular structures in order to obtain the whole spectrum of crystal properties with a better precision.

V. RESULTS OF THE CALCULATIONS FOR KCl AND NaCl CRYSTALS

A. Phonon dispersion curves

In order to check the validity of the pair potentials used in the present study and verify whether our shell parameters are good enough, we have calculated for both crystals phonon dispersion curves in three directions in the BZ: [100] (Γ-Z), [110] (Γ-X), and [111] (Γ-L). The calculations have been done for $T=80$ K for the corresponding experimental spacings[19] $d=5.91$ and 5.29 a.u. for KCl and NaCl, respectively. The results obtained for KCl and NaCl were compared with available experimental inelastic neutron-scattering data[27,28] at the same temperature.

We found that the ppCDN and PIpp demonstrate quite good agreement with the experimental phonon dispersion curves in all symmetry directions in the BZ. However, the results obtained using the TFpp are much worse for the KCl crystal and can even be considered as unsatisfactory: the structure of the phonon curves is not reproduced correctly especially for the [100] and [110]

TABLE II. Shell parameters, obtained by fitting to experimental static, ε_0, and high-frequency, ε_∞, dielectric constants and to the TO phonon frequency, $\omega_{0,\mathrm{op}\perp}$, at $\mathbf{k}=\mathbf{0}$. The calculations were done using the static energy at zero temperature for the experimental (extrapolated to 2 K) crystal spacing d (Ref. 25).

Crystal	d (a.u.)	α_+	α_-	ε_∞	Γ (a.u.)	β (a.u.)	ε_0	$\omega_{0,\mathrm{op}\perp}$ (10^{13} sec^{-1})
KCl	5.8884	4.59	23.48	2.213				
Experimental[a]				2.2			4.49	2.844
Potentials of Catlow *et al.* (ppCDN)					6.59	1.209	4.4896	2.839
Tosi-Fumi potentials (TFpp)					10.98	1.2	4.5141	2.253
ab initio PI potentials (PIpp)					6.5752	1.2	4.4899	2.827
NaCl	5.2704	0.918	22.202	2.483				
Experimental[a]				2.35			5.45	3.353
Potentials of Catlow *et al.* (ppCDN)					677.91	2.32	5.4497	3.271
Tosi-Fumi potentials (TFpp)					810.5	2.32	5.4511	3.066
ab initio PI potentials (PIpp)					675.5	2.32	5.449	3.332

[a]The experimental data used in fitting are 2-K values from Ref. 24.

directions. Besides, the slope of the acoustic branches deviates strongly from the experimental one which reflects the well-known fact[13] that the elastic constants are reproduced badly by these potentials (see also a more detailed discussion below). Lastly, the optical branches are shifted down appreciably because of the unsuccessful fitting of the shell parameters achieved in the case of KCl for these potentials (see Sec. IV and Table II).

Note, however, that peculiarities of the phonon eigenvalues appear not to be so important in calculating crystal thermoelastic properties since all these deviations will have no effect being integrated over the BZ. That is why we can expect that any deviations in the results on the thermodynamic properties displayed by different potentials and discussed below, are the consequences entirely of the corresponding static energies. Thus, on the whole, quite reasonable results are obtained for the phonon frequencies with the help of the shell-like model used in this paper.

B. Zero-pressure general thermodynamic properties

For every type of pair potential we have calculated a number of general thermodynamic properties. We give here in detail only the results for KCl crystal since for NaCl we have obtained a very similar picture. Only the case of zero pressure is considered here. The pressure dependence of thermoelastic properties is discussed in Sec. V G.

We start our consideration from the equation of state of the crystals, i.e., from the dependence of the nearest-neighbor anion-cation distance, d, on the temperature, T. The results of the calculations are plotted in Fig. 1 together with available experimental data taken from Ref. 29. All curves are plotted up to the highest possible temperature until the crystal becomes unstable under zero pressure (for a more detailed discussion on the crystal stability see Sec. V D). We note that the agreement for all the potentials except the PIpp is rather promising through the whole temperature range though at high temperatures the thermal expansion is strongly overestimated. This behavior becomes much more evident if we consider also the temperature derivative of the spacing, i.e., the thermal expansion coefficient, β_T, represented in Fig. 2 (the corresponding experimental data are taken from Refs. 5, 30, and 31). Above $T \simeq 300-400$ K the calculated spacing starts to rise too rapidly in comparison with experimental values. This agrees with a conclusion drawn in Ref. 11. We believe that this discrepancy can be reasonably explained solely by the lack of an anharmonic correction in our calculations. In this respect it is interesting to notice that inclusion of only quartic and squared cubic terms in the Taylor expansion of the potential energy leads to substantially worse results for high T as follows from Ref. 11. Our calculations, made entirely within the simple quasiharmonic approximation appear to be still qualitatively correct even at rather high temperatures though the error becomes larger as the temperature increases. Note that in the case of NaCl crystal the PIpp leads to a better agreement with experimental data on the spacing[32,33] and β_T.[5]

The large deviation for the crystal thermal expansion predicted by the nonempirical PIpp in the case of KCl crystal mainly originates from an overestimated zero-temperature value ($d=6.125$ a.u.) because the general behavior of the curves is reproduced in rather close agreement with the experiment. Note that the original *ab initio* PI method[22] predicts an even worse values for the crystal spacing than the pair potentials produced from it.[21]

For the heat capacity at constant volume C_V, we found very good agreement with available experimental data[34–36] for both crystals and for all types of the pair potentials. We notice also that the theory is consistent with the "classical" prediction $C_V=6k$ at high temperatures. Thus, C_V is too insensitive to the particular form

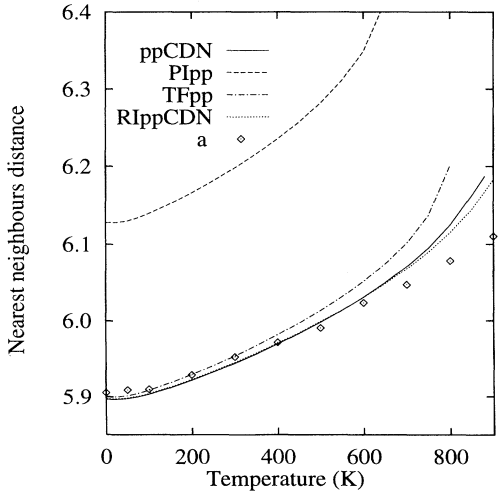

FIG. 1. Anion-cation nearest-neighbor distance (in a.u.) for a KCl crystal calculated for various models (see text). Experimental data are shown by symbols: *a* (Ref. 29).

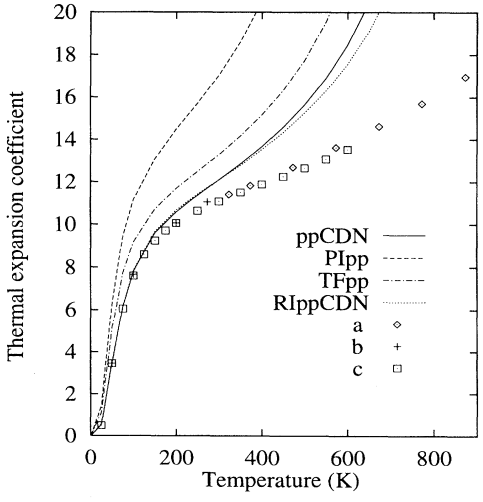

FIG. 2. Thermal expansion coefficient (in units of 10^{-5} K^{-1}) of a KCl crystal calculated for various models (see text). Experimental data represented by symbols are *a* (Ref. 31); *b* (Ref. 30); *c* (Ref. 5).

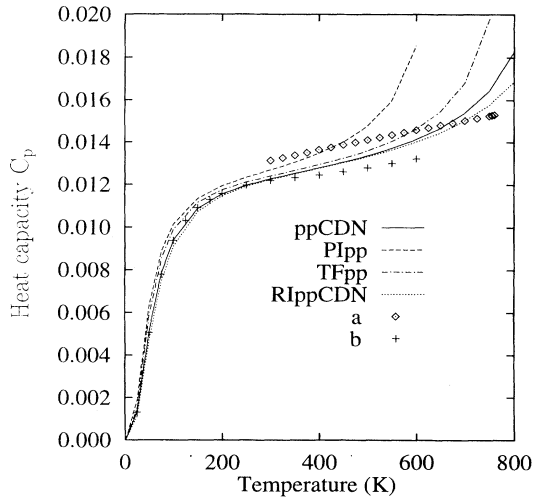

FIG. 3. Heat capacity at constant pressure (in units of kcal $mol^{-1} K^{-1}$) of a KCl crystal calculated for various models (see text). Experimental data represented by symbols are *a* (Ref. 34); *b* (Ref. 5).

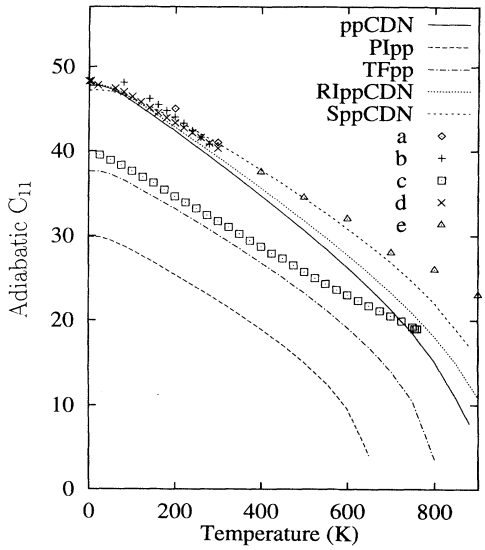

FIG. 4. Adiabatic elastic constant C_{11}^S (in GPa) of a KCl crystal calculated for various models (see text). Experimental data represented by symbols are *a* (Ref. 38); *b* (Ref. 40); *c* (Ref. 34); *d* (Ref. 41); *e* (Ref. 39).

of the pair potentials. On the contrary, the heat capacity at constant pressure, C_p, plotted for KCl crystal in Fig. 3 as an illustration, coincides with experiment[5,34] only for rather small T; at high T it increases too quickly with increasing the temperature. Similarly to the case of the crystal thermal expansion coefficient plotted in Fig. 2, the slope of the C_p is strongly overestimated in our calculations for all three potentials studied though the results for the ppCDN are the best one. This behavior is of the same nature as in the case of β_T and could probably be removed by a proper extension of the quasiharmonic approximation. Note that our results for the thermal expansion and C_p are in close agreement with other quasiharmonic calculations quoted in Ref. 37.

Summing up, we can conclude that both empirical pair potentials considered here, namely, ppCDN and TFpp, demonstrate rather good behavior in comparison with available experimental general thermodynamic data. This is in spite of the fact (mentioned in Sec. V A) that the TFpp fails to give correct phonon dispersion curves. The nonempirical PIpp differ strongly from experiment in thermal expansion data, although it appears to be qualitatively correct.

C. Zero-pressure elastic properties

There are several sets of experimental data[32,34,38–43] on the temperature dependence of individual zero-pressure adiabatic elastic constants of alkali halides. It is evident that there is a substantial difference in experimental data especially for KCl. Nevertheless, qualitative features of the elastic constants are the same for both crystals.

Our theoretical curves for both crystals are similar and we represent here in Figs. 4–6 our results only for KCl. All three potentials give qualitatively correct dependence on T. Both C_{11}^S and C_{44}^S decrease with temperature. Unlike C_{44}^S, the constant C_{11}^S tends to achieve a zero value at the boundary of the crystal stability at high enough T (see also Sec. V D). The slope for C_{11}^S is very close the experimental data in the case of KCl but was found to be slightly overestimated for NaCl at high temperatures. The agreement with experiment for C_{44}^S turned out to be al-

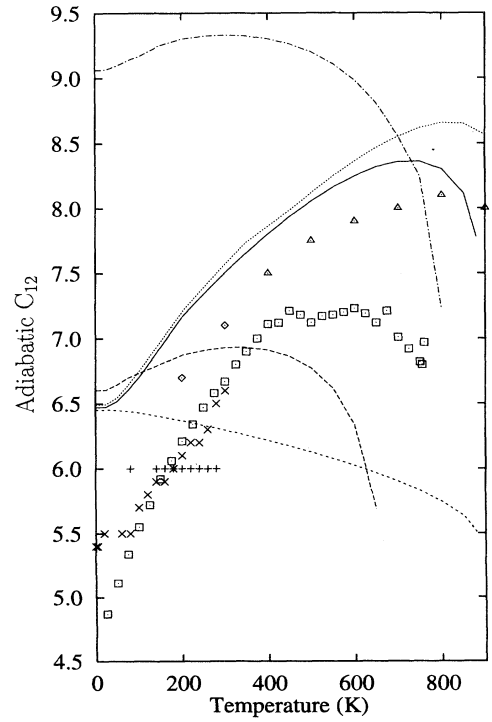

FIG. 5. Adiabatic elastic constant C_{12}^S (in GPa) of a KCl crystal calculated for varoius models (see text). Notations are the same as in Fig. 4.

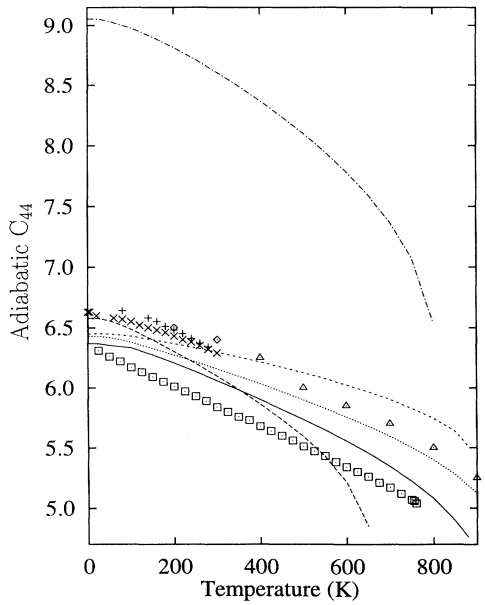

FIG. 6. Adiabatic elastic contant C_{44}^S (in GPa) of a KCl crystal calculated for various models (see text). Notations are the same as in Fig. 4.

most excellent for the ppCDN for both crystals. The PIpp give results which are close to experiment for KCl but are strongly shifted upward with respect to the experimental data in the case of NaCl. As was expected,[13] the agreement with the experiment for the TFpp is generally poor especially for C_{44}^S in KCl.

As follows from the experimental data quoted above, at low temperatures the elastic constant C_{12}^S must have a positive slope with a peak near 600 K (NaCl) and 800 K (KCl); this slope in the case of NaCl is smaller than in the case of KCl. Qualitatively both these features are reproduced well in our theoretical curves especially for the ppCDN, see Fig. 5 as an illustration. The quantitative agreement for the TFpp and PIpp with the experiment is generally worse.

We should emphasize that our results for the TFpp are quantitatively different from those originally published in Ref. 13. We think that this discrepancy is explained, first of all, by an insufficient precision of the calculations made in Ref. 13, i.e., by a small number of **k** points in the BZ used in calculating the free energy. Indeed, as was pointed out above in Sec. IV, the shear elastic constant C_{12}^S turns out to be very sensitive to the number of special points used in the BZ summation, especially at high temperatures. Our calculations show that the right (high-temperature) tail of the C_{12}^S curve tends upwards while further increasing the precision in the BZ summation in comparison with that used in the present calculations (28 special points). Besides, in comparison with Ref. 13, we have used equilibrium spacings obtained entirely within the quasiharmonic approximation.

In spite of the fact that our calculations were done within the model of central pairwise forces, the phonon contribution used in calculating the free energy and its derivatives is of a many-body nature. This term is only one which has a T dependence and thus leads to the crystal thermal expansion. However, it was found to be important for the elastic properties as well. In order to clarify this point let us consider a special model for the KCl crystal in which static elastic constants are calculated for the crystal geometries found in our full quasiharmonic calculations. The elastic constants calculated in this way for the ppCDN are plotted in Figs. 4–6. We shall refer this model as to the static ppCDN (SppCDN). Let us compare results obtained with (ppCDN) and without (SppCDN) the phonon contributions to the elastic constants. It is seen that this contribution is a small positive slowly increasing function of T in the case of C_{11}^S and C_{44}^S and does not change their qualitative behavior. On the contrary, in the case of C_{12}^S the thermal contribution is found to be very large positive function of T with a nontrivial behavior and is uniquely responsible for the positive slope of the shear constant C_{12}^S observed in the experiment at small and intermediate T. Thus, the thermal contribution to the elastic constants (i.e., the phonon part of the free energy) turned out to be very important in contrast to the conclusion drawn in Ref. 13.

It is well known that the Cauchy condition $C_{44}^S = C_{12}^S$ is violated in the case of alkali halides throughout the whole range of the stability of the crystals. In particular, at small T the shear constant C_{12}^S is less than C_{44}^S whereas at some temperature (about 200 K for KCl and 300 K for NaCl) this inequality is reversed. Then C_{44}^S continues to decrease whereas C_{12}^S continues to rise until it reaches a maximum and then decreases at higher T. Although our calculations fairly yield different C_{12}^S and C_{44}^S (because of the quasiharmonic approximation), we do not observe at all this property for KCl no matter what type of potentials has been used, i.e., we have $C_{12}^S > C_{44}^S$ for the whole range of T. In the case of NaCl $C_{12}^S < C_{44}^S$ is only slightly evident for very small T. Indeed, for this crystal we have obtained a very small positive difference $C_{44}^S - C_{12}^S$ for $T=0$ K (about 0.1–0.2 GPa) instead of a value of the order of several GPa's observed experimentally. Note that our difference at this temperature follows entirely from the contribution of zero phonons to the Helmholtz free energy which appears to be very small. Besides, anharmonic corrections can also be disregarded at small T. So, as was fairly mentioned in Ref. 12, the large positive difference between C_{44}^S and C_{12}^S must originate from three-body forces which are absent in the present calculations. Thus, our analysis argues once more that the three-body forces must be quite important for KCl and NaCl crystals in order to explain the correct sign of the violation of the Cauchy relation.

In contrast to other general thermodynamic properties, the elastic constants appear to be very sensitive to the particular potentials used in the calculations. This is because of specific anisotropic distortions from which the crystals suffer in every case: the symmetrical neighborhood of every atom is changed substantially during such deformations. Some examples of such deformations were considered in Refs. 13, 44, and 45. The point that the elastic constants require anisotropic strain derivatives of

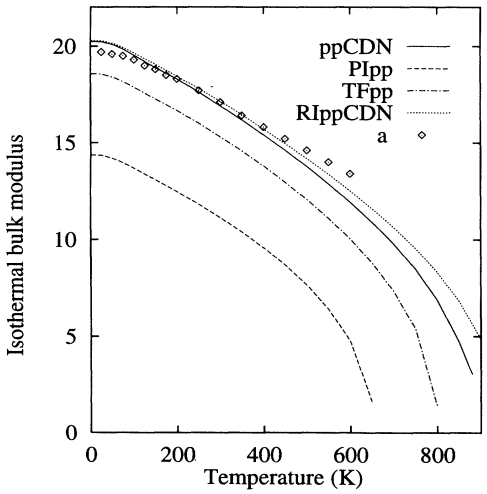

FIG. 7. Isothermal bulk modulus (in GPa) of a KCl crystal calculated for various models (see text). Experimental data represented by symbols are *a* (Ref. 5).

the free energy has been repeatedly stated in the literature (see, for instance, Refs. 13 and 14). That is why simple models which do not take this circumstance into account are not able to explain such a nontrivial elastic behavior of the crystals. In particular, within the effective one-frequency Einstein model[46] this is not possible because of the crystal anisotropy which is not reproduced correctly by this approximation. Besides, the symmetric Einstein[10] model made in the framework of the self-consistent phonon formalism also fails to explain the violation of the Cauchy condition as well as the positive slope for the C_{12}^S observed at not very high T.

The isothermal, B_T, and adiabatic, B_S, bulk modulus reflect overall behavior of the corresponding elastic constants. The isothermal bulk modulus of KCl crystal is plotted in Fig. 7 as an example. Both properties have a tendency to decrease with increasing temperature because the crystal gradually loses its stability.[5] For both crystals and for both constants all the potentials result in almost similar slopes. However, they appear to be overestimated if we compare with the experiment,[5,42] especially in the case of the B_S. As in the previous cases, the agreement with the experiment is rather good for all models under question except the case of the PIpp for the KCl crystal when the agreement is poor. Generally, overall accord with the experiment for the isothermal bulk modulus is substantially better than for the adiabatic one.

D. An analysis of the crystal stability at high temperatures near the melting point

Let us discuss now how a crystal approaches a point where it loses its stability, presumably because of melting.[9] In this respect it would seem to be reasonable first to study the question of crystal isotropy. It is known that a substance becomes isotropic when the speed of sound is independent of the direction of the propagation. This happens when $C_{11}-C_{12}=2C_{44}$ (both for adiabatic and isothermal waves). We have checked this equality in our case. We found that for all potentials and for both crystals the ratio of $C_{11}-C_{12}$ and $2C_{44}$ is positive for small T, but at some specific T this inequality changes its sign. This crucial temperature is greater for KCl than for NaCl by an amount of 100–200 K but depends strongly on the type of the potentials. Thus, in agreement with other calculations,[44] both crystals do not behave as isotropic media while T tends to the melting temperature.

Moreover, we have obtained a very fast decrease to zero of the isothermal C_{11}^T and C_{12}^T (and therefore, the same trend for B_T) with increasing T whereas the elastic constant C_{44} does not display this behavior. Note that adiabatic elastic constants do not decrease so sharply because of the large thermal contribution which increases with T. We have found that at some critical temperature which is close (but not equal) to the point where $C_{11}^T=0$, the crystals show some kind of a catastrophic behavior. In order to illustrate this point, let us consider a KCl crystal with ppCDN as an example.

As is known,[5] a cubic crystal is stable, i.e., the corresponding Hessian matrix of the free-energy second-order derivatives is positive definite, when the following conditions are fulfilled simultaneously: $C_{11}+2C_{12}>0$, $C_{11}>C_{12}$ and $C_{44}>0$. Note that the first inequality can be replaced by $C_{11}>0$ because of the second one. The typical behavior of the KCl crystal free energy is shown in Fig. 8 by the first curve which corresponds to $T=880$ K (similar behavior was obtained also in Ref. 9). The free energy has a minima at some spacing d_0. The corresponding Hessian matrix is positive definite so that the isothermal elastic constants listed in Table III in detail satisfy the stability conditions given above. When $d<d_0$ the free energy increases rather quickly. The region $d<d_0$ belongs to the case of higher (nonzero) pressures. However, when $d>d_0$, the free energy at first increases (an unphysical region of negative pressures), then it

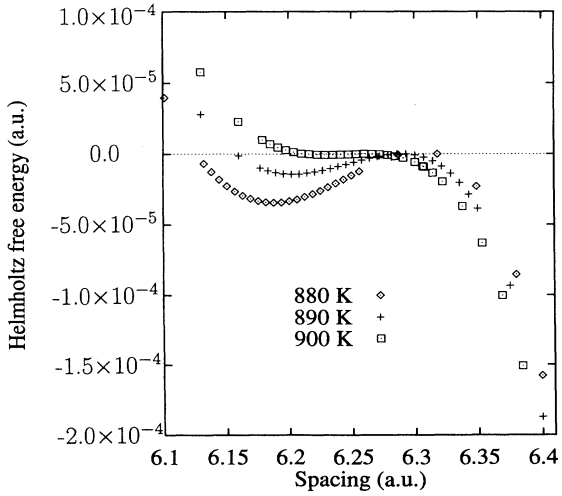

FIG. 8. Relative Helmholtz free energies of a KCl crystal (in a.u.) calculated using ppCDN for 880, 890, and 900 K.

TABLE III. Elastic properties of a KCl crystal calculated by means of the ppCDN at the temperatures which are close to our prediction of the melting temperature.

Property	$T=880$ K	$T=890$ K	$T=900$ K
d[a], a.u.	6.187 73	6.205 10	6.228 83
C_{11}^T, GPa	3.036 5	1.226 34	−2.631 6
C_{12}^T, GPa	3.029 35	2.090 24	2.044 91
C_{44}^T, GPa	4.757 76	4.692 14	4.558 95
C_{11}^S, GPa	7.786 83	6.181 92	2.879 12
C_{12}^S, GPa	7.779 68	7.045 83	7.332 35
B_T, GPa	3.042 57	1.806 38	0.498 82
B_S, GPa	7.792 9	6.761 97	5.860 11

[a]The nearest anion-cation distance corresponding to the free-energy minima.

passes through a maximum and abruptly decreases until, at some critical spacing, d_c, the phonon frequencies become imaginary and therefore the crystal ceases to exist. As the temperature decreases, the minima becomes deeper and the barrier higher. However, as is clear from other curves plotted in Fig. 8, as the temperature increases, the minima becomes more shallow and the barrier gradually disappears.

Let us consider now what happens with the crystal stability as the temperature increases from 880 to 900 K (Fig. 8). Corresponding elastic constants are listed in Table III. It is seen that the isothermal elastic constant C_{11}^T changes catastrophically quickly while the temperature increases by only 20°. So, already at $T=890$ K the stability condition $C_{11}^T > C_{12}^T$ is violated. It means that the Hessian matrix in the minima is negative definite and we have here actually a saddle point. At somewhat higher T (near 900 K) the first condition is also violated (i.e., C_{11}^T becomes negative) and the saddle point almost disappears. So, at some critical temperature (the critical temperature of the catastrophe), which is close to 890 K in our calculations for the particular case considered, the crystal becomes completely unstable under zero pressure and undergoes a transition to the region where its energy tends to large negative values. In other words, the crystal transforms to another structure which has substantially higher spacing and imaginary phonon frequencies. It is reasonable to expect that the crystal starts to melt and that this critical T can be thought of as the melting temperature. It is worthwhile mentioning here that the adiabatic elastic constants are still quite large even at 900 K. However, as is seen from Table III, they generally also do not satisfy the stability condition $C_{11}^S > C_{12}^S$, starting from the same $T=890$ K.

Thus, we see from our calculations that the KCl crystal becomes unstable due to the failure of the condition $C_{11}^T > C_{12}^T$ (or $C_{11}^S > C_{12}^S$). The real critical behavior displays only one elastic constant, namely, C_{11}^T, which actually controls the transition process and plays a major role in the melting. In this respect we would like to emphasize, as follows from our calculations, that B_T reaches zero after the difference $C_{11}^T - C_{12}^T$ becomes zero. Note that this is in contrast to a conclusion drawn in Ref. 9 where the author insisted that the condition $B_T \Longrightarrow 0$ occurs first as T increases.

Another important consequence is that the catastrophe begins its work of destroying the crystal even earlier than the minimum in the free energy versus spacing (i.e, versus volume) disappears completely. This means, that in order to estimate the melting temperature, a detailed analysis of the dependence of the Hessian matrix on the path of the transition is necessary, and an analysis based only on the volume dependence of the free energy[9] may be insufficient and may lead to a somewhat overestimated transition temperature.

However, the corresponding critical temperatures predicted in our calculations [about 900, 700, 850 K (KCl) and 700, 650, 700 (NaCl) for the ppCDN, TFpp, and PIpp, respectively] turned out to be far below the experimental melting temperatures (1077 K for NaCl and 1045 K for KCl). Moreover, we found an incorrect trend for both crystals. We expect this is the consequence of the quasiharmonic approximation which likely does not work properly at T greater than half of the melting temperature.[11] Nevertheless, it is highly satisfactory to note that this approximation is able to give a reasonable qualitative physical picture even up to very high temperatures.

E. Rigid-ion model

It is known[5,7,8] that in the case of such centrosymmetric crystals as alkali halides, shells do not contribute to the elastic properties of the static lattice. However, as far as quasiharmonic theory based on the shell-like model is concerned, the shells affect the crystal phonons, and, in this way, indirectly influence all the crystal thermodynamic properties.

In order to check the role of the shells in crystal thermoelastic properties, we have also considered a rigid-ion KCl crystal with the ppCDN. We shall call this mode RIppCDN in that which follows. We found that the acoustic branches of the phonon dispersion curves calculated in this model are reproduced rather well in the long-wavelength region. This is because of the fact, already mentioned above, that the shells do not contribute to static elastic constants for centrosymmetric crystals. At the same time, the optical branches turn out to be completely wrong because of the failure of the model to give correct long-wavelength optical frequencies. Nevertheless, as follows from the results of the calculations presented in Figs. 1–7, except very high T, all the general thermodynamic properties are revealed to be practically indistinguishable in both models when the shells are included (solid lines) and are not included (dotted lines). This happens because in calculating the integral over the BZ all the peculiarities of the phonon frequencies become unimportant. So, the role of the shells appear to be insignificant in calculating crystal thermodynamics, as was expected.

F. Crystal dielectric properties

It is known that alkali halides are centrosymmetric crystals and therefore do not show piezoelectric properties. In Figs. 9 and 10 we have plotted calculated and experimental[24] low- (static) and high-frequency dielectric constants of KCl crystal under zero pressure against T.

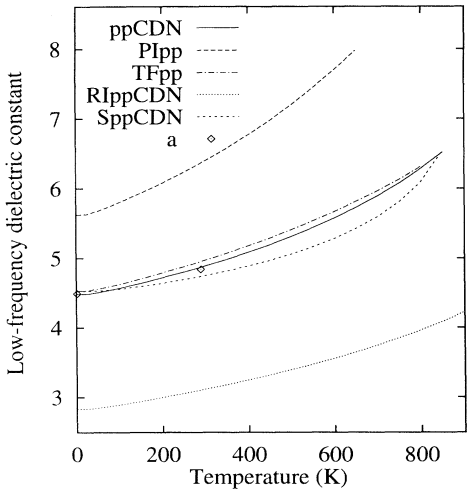

FIG. 9. Low-frequency dielectric constant of a KCl crystal calculated for various models. Experimental data represented by symbols are *a* (Ref. 24).

Our results for all three potentials are given there.

First of all we would like to stress that in all cases considered, we have obtained correct qualitative behavior of both ε_0 and ε_∞. Namely, the static constant grows together with T, while ε_∞ decreases. Moreover, the agreement for the ppCDN and TFpp for KCl is almost perfect whereas the PIpp show a large constant shift (about 10% for ε_∞ and 20% for ε_0) from the experimental points. In the case of NaCl the quantitative agreement of ε_0 with experiment[24,47] is worse for all the potentials examined here; however, deviations for ε_∞ from the experiment[24] are rather small (about 2.5–6%). Generally, we can say that the results obtained with the ppCDN are the best.

In the case of KCl crystal and for the ppCDN two additional models have been also examined (Fig. 9): (a) the rigid-ion approximation (RIppCDN) and (b) the model in which the ε_0 was calculated from the static energy for correct quasiharmonic spacings (SppCDN). Since there is no thermal contribution to ε_∞, we have obtained $\varepsilon_\infty = 1$ in the former case and the same result for it as in the quasiharmonic approximation in latter case. However,

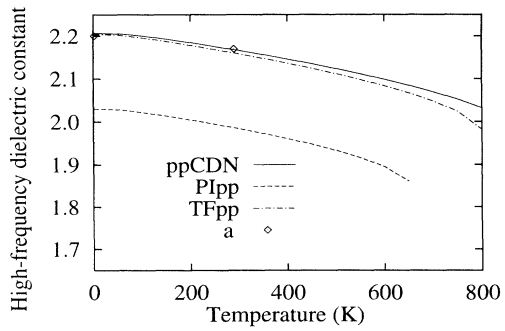

FIG. 10. High-frequency dielectric constant of a KCl crystal calculated for various models. Experimental data represented by symbols are *a* (Ref. 24).

the static dielectric constant has some contribution from the phonons through the second-order internal strain derivatives (see I). From the curves plotted in Fig. 9 we observe a well-known result that the rigid-ion model strongly underestimates ε_0. At the same time, the static energy calculations give surprisingly good results. This indicates that there is quite a small contribution to the internal strain derivatives from the phonons, and ε_0 is defined almost exclusively by the static energy calculated for the correct crystal structure.

The results obtained for the dielectric properties show that our core-shell potentials (see Sec. IV) are able to reproduce correctly the dielectric properties of the crystals throughout the wide range of T. Another conclusion that can be drawn from our calculations is that the quasiharmonic approximation is found to be valid up to very high T.

G. Pressure dependence of thermoelastic and dielectric properties

So far we have considered crystal properties only under zero pressure. However, the pressure dependence of thermoelastic properties is also of great interest, since the role of anharmonicity becomes less important as the crystal is compressed.[12] This is because of atomic displacements which are smaller in the crystal under pressure. Thus, the pressure dependence of thermoelastic properties calculated in the quasiharmonic approximation would be an excellent test of the validity of the pair potentials.

Two types of experimental data are verified in this section: (i) room-temperature (293 K) measurements of the elastic constants of NaCl for pressures up to 10 GPa,[48] and (ii) high-temperature (300, 550, and 800 K) measurements of the elastic constants and of the thermal expansion coefficient for a comparatively narrow range of pressures (up to only 1 GPa) published in Ref. 43. Note that in both cases we should calculate the adiabatic stiffneses B_{ij}^S instead of the adiabatic elastic constants since it is the former that actually define the speed of the sound in the compressed crystal. This point has been extensively clarified in the literature.[5]

We have made a special set of calculations for NaCl at 293 K over a wide range of crystal spacings in order to cover a range of pressures up to 10 GPa. Generally, for the adiabatic stiffnesses B_{11}^S, B_{12}^S, and B_{44}^S we have obtained almost linear pressure dependencies with the slopes summarized in Table IV. The experimental

TABLE IV. Pressure derivatives of adiabatic stiffnesses of NaCl crystal at $T=293$ K calculated by means of different pair potentials.

	$\frac{\partial B_{11}^S}{\partial P}$	$\frac{\partial B_{12}^S}{\partial P}$	$\frac{\partial B_{44}^S}{\partial P}$
Experimental data (Ref. 48)	11.11	1.67	0.42
ppCDN	9.6	1.65	−0.56
TFpp	8.0	2.05	0.12
PIpp	11.1	1.40	−0.43

curves[48] are also linear and their slopes are also given in Table IV. We see that except for B_{44}^S our results obtained with all three potentials are in reasonable agreement with the experiment. Moreover, the PIpp give slopes which are very close to experiment. Unfortunately, the slopes for B_{44}^S are of an opposite sign for the ppCDN and PIpp. The slope obtained with the TFpp is positive (as in the experiment) but is underestimated by more than a factor of 3.

Some of our high-temperature results for pressures up to 4 GPa are represented in Figs. 11–14 together with experimental data (up to 1 GPa) taken from Ref. 43. Analyzing the results of the calculations, we would like to notice the following.

(1) The thermal expansion coefficient (Fig. 11) decreases with P for each of the pair potentials; besides, there is some appreciable shift up of every curve as the temperature increases. These qualitative features are also observed in the experiment.

(2) For every potential there is a linear growth of B_{11}^S (Fig. 12) with P which is almost the same for all three T studied; the curves are shifted down as the temperature increases in accord with the experimental data although this shift is overestimated. Note that we have obtained similar curves for B_T and B_S as well.

(3) B_{12}^S (Fig. 13) displays a positive slope with P for every T. For small pressures

$$B_{12}^S(T=800) < B_{12}^S(T=550) < B_{12}^S(T=300)$$

in the cases of the ppCDN and PIpp. However, as P increases, these inequalities are changed to

$$B_{12}^S(T=300) < B_{12}^S(T=550) < B_{12}^S(T=800) .$$

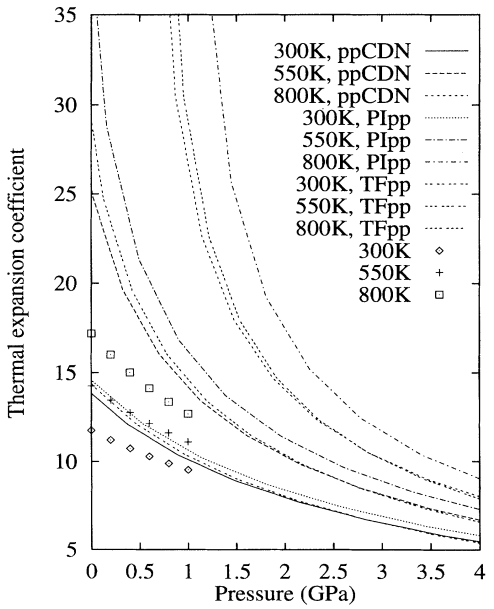

FIG. 11. Pressure dependence of the NaCl thermal expansion coefficient (in units of 10^{-5} K^{-1}) calculated with the help of different potentials for 300, 550, and 800 K. Experimental data from Ref. 43 are shown by symbols.

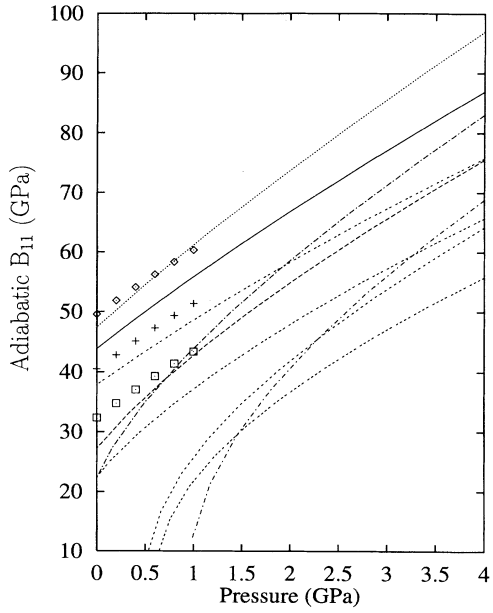

FIG. 12. Pressure dependence of the adiabatic stiffness B_{11}^S (in GPa) of a NaCl crystal calculated with the help of different potentials for 300, 550, and 800 K. Notations are the same as in Fig. 11.

In the case of the TFpp the latter inequality is not broken throughout the whole pressure range. On the other hand, according to the experiment, we have

$$B_{12}^S(T=300) < B_{12}^S(T=800) < B_{12}^S(T=550)$$

for small P and the inequality

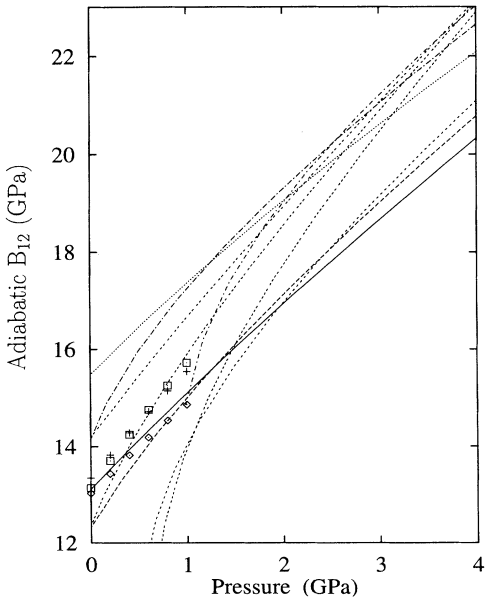

FIG. 13. Pressure dependence of the adiabatic stiffness B_{12}^S (in GPa) of a NaCl crystal calculated with the help of different potentials for 300, 550, and 800 K. Notations are the same as in Fig. 11.

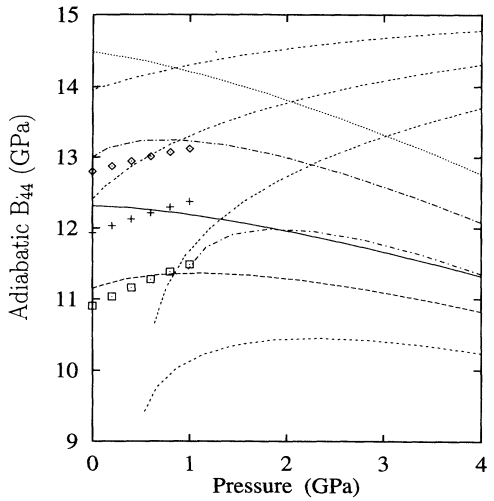

FIG. 14. Pressure dependence of the adiabatic stiffness B_{44}^S (in GPa) of a NaCl crystal calculated with the help of different potentials for 300, 550, and 800 K. Notations are the same as in Fig. 11.

$$B_{12}^S(T=300) < B_{12}^S(T=550) < B_{12}^S(T=800)$$

for large P. Thus, the pair potentials studied in this work do not give correct qualitative behavior with T for this shear elastic property. This is because of the complex character of the shear elastic constants with T which has been discussed already in Sec. V C: all the pair potentials do not reproduce quantitatively experimental data for C_{12}^S even for zero pressure. We should point out, however, that for small pressures our results should be corrected by proper inclusion of the anharmonic contributions, especially in the $T=800$ K case.

(4) B_{44}^S (Fig. 14) decreases with temperature throughout the whole range of pressures in accord with experiment; however, as was already mentioned above in this section, we have obtained negative slopes with pressure for all potentials except the TFpp which disagrees with the experiment.

Generally, the results of our calculations presented in this section dealing with the simultaneous pressure and temperature dependence of the elastic properties of NaCl crystal provide us with additional information about the existing pair potentials. We have shown that even the ppCDN which were found to be the most successful for both crystals for the zero-pressure properties (i.e., for larger spacings), show several disagreements with the experiment in the shear elastic constants as the pressure increases (i.e., the spacing becomes smaller).

VI. CONCLUSIONS

A general theory proposed in I and discussed in detail here gives a unified method for studying a wide range of thermoelastic and dielectric properties of perfect shell-like-model crystals governing by pairwise forces. A numerical method elaborated by us has been implemented in a computer code DYNAM which is written for arbitrary crystal symmetry and structure. If the space group and a set of pair potentials between atoms in the crystal are known, it is possible to fit corresponding core-shell and (if it is necessary) shell-shell short-range potentials to proper experimental data and then calculate a number of desired crystal properties under any conditions of stress and temperature.

The temperature dependence of a number of thermoelastic and dielectric properties of perfect KCl and NaCl ionic crystals studied in this paper have been calculated from several pair potentials. The empirical potentials of Catlow *et al.*[19] demonstrate on average an overall agreement with available experimental data on the temperature dependence under zero pressure for all properties considered. The potentials of Tosi and Fumi[20] allow one to reproduce closely only general thermodynamic and dielectric data, but they fail to give good elastic constants (cf. Ref. 13). The *ab initio* PI pair potentials[21] demonstrate reasonable quantitative thermal contributions and result in a qualitatively correct physical picture for almost all properties studied. However, these potentials display poor static properties and therefore their final results are usually far from the experimental data.

In agreement with other calculations[9,11,44] we found that the quasiharmonic approximation is able to give correct qualitative results throughout the whole temperature range, even up to the melting point. However, in order to explain existing experimental data at rather high T, greater than about half of the melting temperature, one needs to include proper anharmonic corrections which were found to be large in KCl and NaCl crystals in contrast to the results of Ref. 13. Otherwise, the results of the calculations may be far from those observed experimentally.

In contrast to a conclusion drawn in Ref. 13 we have shown that the violation of the Cauchy relation at small temperatures can be attributed only to the three-body-like interactions in the crystals. This is also in agreement with other theoretical works.[12]

However, our study of the simultaneous pressure and temperature behavior of the elastic properties of NaCl crystal demonstrates large deviations between experimental and theoretical elastic constants (stiffnesses). This shows that further work has to be done in order to improve existing pair potentials especially in the region of small spacings. We think that this can be done by a least-squares-fit method based on a wider set of experimental information than it is usually done, i.e., taking into account also data for nonzero temperatures and especially for nonzero pressures. We hope that our computer code could be helpful and useful in treating this routine problem.

ACKNOWLEDGMENTS

I would like to express my warmest thanks to all my colleagues in the quantum-chemistry group of the University of Oveido, led by Prof. L. Pueyo, for their constant interest in this work, a number of useful discussions, and also for the whole encouraging atmosphere

which has helped me to work on this problem. The author is grateful to the Centro de Cálculo Científico, Universidad de Oveido, for the CONVEX facility in which all the calculations have been done. I would like also to express my gratitude to the Direccion General de Investigacion Científica y Técnica (Spain) for Grants Nos. SAB92-0226 and SAB94-0064 allowing me to finish this work.

---

*On leave from Physical-Chemical Institute, University of Latvia, Riga, Latvia. Present address: Department of Physics, University of Keele, Newcastle-under-Lyme, Staffordshire, ST5 5BG, UK.

[1]L. N. Kantorovich, preceding paper, Phys. Rev. B **51**, 3520 (1995).

[2]D. C. Wallace, in *Solid State Physics,* edited by F. Seitz and D. Turnbull (Academic, New York, 1970), Vol. 25, p. 301.

[3]J. A. Reissland, *The Physics of Phonons* (Wiley, London, 1973).

[4]K. B. Tolpygo, Izv. Acad. Nauk SSSR Ser. Fiz. **24**, 177 (1960); K. B. Tolpygo, Usp. Fiz. Nauk **74**, 269 (1961) [Sov. Phys. Usp. **4**, 485 (1961)]; K. B. Tolpygo, Phys. Status Solidi B **56**, 591 (1973).

[5]D. C. Wallace, *Thermodynamics of Crystals* (Wiley, New York, 1972).

[6]A. M. Stoneham, *Theory of Defects in Solids* (Clarendon, Oxford, 1975).

[7]A. A. Maradudin, E. W. Montroll, G. H. Weiss, and I. P. Ipatova, *Theory of Lattice Dynamics in the Harmonic Approximation* (Academic, New York, 1969).

[8]A. D. B. Woods, W. Cochran, and B. N. Brockhouse, Phys. Rev. **119**, 980 (1960).

[9]L. L. Boyer, Phys. Rev. B **23**, 3673 (1981).

[10]S. Nambu and M. Oiji, J. Phys. Soc. Jpn. **59**, 4366 (1990).

[11]Z. Gong, G. K. Horton, and E. R. Cowley, Phys. Rev. B **38**, 10 820 (1988).

[12]E. R. Cowley, Z. Gong, and G. K. Horton, Phys. Rev. B **41**, 2150 (1990).

[13]F. H. Ree and A. C. Holt, Phys. Rev. B **8**, 826 (1973).

[14]V. V. Mitskevich, Sov. Phys. Solid State **3**, 2202 (1962); **3**, 2211 (1962).

[15]R. A. Evarestov and V. P. Smirnov, Phys. Status Solidi B **119**, 9 (1983).

[16]C. R. A. Catlow and W. C. Mackrodt, in *Computer Simulation of Solids,* edited by C. R. A. Catlow and W. C. Mackrodt, Lecture Notes in Physics, Vol. 166 (Springer-Verlag, Berlin, 1982), p. 3.

[17]A. G. McLellan, *The Classical Thermodynamics of Deformable Material* (Cambridge University Press, Cambridge, 1980).

[18]H. I. Monkhorst and J. D. Pack, Phys. Rev. B **13**, 5188 (1976).

[19]C. R. C. Catlow, K. M. Diller, and M. J. Norgett, J. Phys. C **10**, 1395 (1977).

[20]F. H. Fumi and M P. Tosi, J. Phys. Chem. Solids **25**, 31 (1964); **25**, 45 (1964).

[21]J. M. Recio, E. Francisco, M. Florez, and A. Martin Pendas, J. Phys. Condens. Matter **5**, 4975 (1993).

[22]V. Luaña and L. Pueyo, Phys. Rev. B **41**, 3800 (1990).

[23]G. D. Mahan, Phys. Rev. B **34**, 4235 (1986).

[24]R. P. Lowndes and D. H. Martin, Proc. R. Soc. London Ser. A **308**, 473 (1969).

[25]P. B. Ghate, Phys. Rev. **139**, A1666 (1965).

[26]R. H. Lyddane, R. G. Sachs, and E. Teller, Phys. Rev. **59**, 73 (1941).

[27]G. Raunio and L. Almqvist, Phys. Status Solidi **33**, 209 (1969).

[28]G. Raunio, L. Almqvist, and R. Stedman, Phys. Rev. **178**, 1496 (1969).

[29]See, for example, Ref. 10.

[30]P. P. Meincke and G. M. Graham, Can. J. Phys. **43**, 1853 (1965).

[31]A. J. Leadbeter and D. M. T. Newsham, J. Phys. C **2**, 210 (1969).

[32]J. T. Lewis, A. Lehoczky, and C. V. Briscoe, Phys. Rev. **161**, 877 (1967).

[33]*American Institute of Physics Handbook,* edited by D. E. Gray, 3rd ed. (McGraw-Hill, New York, 1972).

[34]F. D. Enck, Phys. Rev. **119**, 1873 (1960).

[35]W. T. Berg and J. A. Morrison, Proc. R. Soc. London Ser. A **242**, 467 (1957).

[36]Clusius, Goldman and Perlick, Z. Naturforsch Teil A **4**, 424 (1949).

[37]H. R. Glyde and M. L. Klein, CRC Critical Rev. Solid State Sci. **1**, 181 (1971).

[38]R. A. Bartels and D. E. Schuele, J. Phys. Chem. Solids **26**, 537 (1965).

[39]Q. D. Slagle and H. A. McKinstry, J. Appl. Phys. **38**, 437 (1967).

[40]M. A. Durand, Phys. Rev. **50**, 449 (1936).

[41]M. H. Norwood and C. V. Briscoe, Phys. Rev. **112**, 45 (1958).

[42]W. C. Overton and R. T. Swim, Phys. Rev. **84**, 758 (1951).

[43]H. Spetzler, C. G. Sammis, and R. J. O'Connel, J. Phys. Chem. Solids **33**, 1727 (1972).

[44]T. H. Kwon, Solid State Commun. **82**, 1001 (1992); S. C. Kim and T. H. Kwon, Phys. Rev. B **45**, 2105 (1992); T. H. Kwon, S. D. Kwon, Z. H. Yoon, Y. K. Sohn, and S. C. Kim, Physica B **183**, 75 (1993); S. C. Kim and T. H. Kwon, J. Phys. Chem. Solids **53**, 539 (1992).

[45]M. Catti, R. Dovesi, A. Pavese, and V. R. Saunders, J. Phys. Condens. Matter **3**, 4151 (1991).

[46]G. Leibfried and W. Ludwig, in *Solid State Physics,* edited by F. Seitz and D. Turnbull (Academic, New York, 1961), Vol. 12, p. 276; R. A. Cowley, Adv. Phys. **12**, 421 (1963).

[47]J. C. Owens, Phys. Rev. **181**, 1228 (1969).

[48]H. Kinoshita, N. Hamaya, and H. Fujisawa, J. Phys. Earth **27**, 337 (1979).